Oncogene (2007) 26, 6406–6419

www.nature.com/onc

ORIGINAL ARTICLE

ERα–CITED1 co-regulated genes expressed during pubertal mammary gland development: implications for breast cancer prognosis

J McBryan[1], J Howlin[1,4], PA Kenny[2], T Shioda[3] and F Martin[1]

[1]UCD School of Biomolecular and Biomedical Science, Conway Institute, University College Dublin, Belfield, Ireland; [2]Lawrence Berkeley National Laboratory, University of California, Berkeley, CA, USA; [3]Laboratory of Tumour Biology, Massachusetts General Hospital Cancer Centre, Charlestown, Massachusetts, USA

Expression microarray analysis identified over 930 genes regulated during puberty in the mouse mammary gland. Most prominent were genes whose expression increased in parallel with pubertal development and remained high thereafter. Members of the Wnt, transforming growth factor-β and oestrogen-signalling pathways were significantly overrepresented. Comparison to expression data from CITED1 knockout mice identified a subset of oestrogen-responsive genes displaying altered expression in the absence of CITED1. Included in this subset are stanniocalcin2 (Stc2) and amphiregulin (Areg). Chromatin immunoprecipitation revealed that ERα binds to oestrogen response elements in both the Stc2 and Areg genes in the mammary gland during puberty. Additionally, CITED1 and ERα localize to the same epithelial cells of the pubertal mammary gland, supporting a role for interaction of these two proteins during normal development. In a human breast cancer data set, expression of Stc2, Areg and CITED1 parallel that of ERα. Similar to ERα, CITED1 expression correlates with good outcome in breast cancer, implying that potential maintenance of the ERα–CITED1 co-regulated signalling pathway in breast tumours can indicate good prognosis.
Oncogene (2007) **26,** 6406–6419; doi:10.1038/sj.onc.1210468; published online 7 May 2007

Keywords: mammary gland; puberty; development; CITEDI; ERα

Introduction

Pubertal mammary gland development is a naturally occurring period of rapid, highly controlled growth. In response to hormones, puberty sees the formation of a mature gland through ductal morphogenesis and invasion of the fat pad by an expanding system of branched epithelial ducts. At the tip of the growing ducts are terminal end bud (TEB) structures. In the mouse, 'a remarkable rate of ductal elongation of about 0.5 mm/day' can be observed when TEBs are present (Daniel and Silberstein, 2000). TEBs are a unique feature and a driving force of pubertal ductal morphogenesis. TEBs consist of a single outer layer of undifferentiated cells known as cap cells and multiple inner layers of body cells. The cap cells are considered to be the pleuripotential stem cells of the developing gland (Williams and Daniel, 1983). The cap cell layer is continuous with the myoepithelium of the subtending duct (Williams and Daniel, 1983). The body cells closest to the cap cell layer are highly proliferative, support outward growth of the duct and give rise to epithelial cells of the mature duct. The body cells furthest from the cap cell layer undergo apoptosis, an important feature facilitating formation of the ductal lumen (Humphreys *et al*., 1996). TEBs regress when epithelial ducts reach the edges of the fat pad and are absent from the mature adult gland.

The functional purpose of pubertal mammary gland development is to prepare the gland for subsequent growth and differentiation during pregnancy. In the absence of a subsequent pregnancy, the nulliparous gland is left more susceptible to cancer than a parous gland (Russo *et al*., 2005). It is thought that the nulliparous gland, with its lack of differentiation, has a greater proportion of undifferentiated stem cells than the gland at any other time, which may account for later transformation (Ball, 1998; Russo *et al*., 2005). We therefore hypothesize that the mechanisms of development employed during puberty, which are required to reach the adult state, may have relevance for cancer susceptibility and/or tumour progression.

Expression microarray analysis of developmental time courses is an effective way of identifying key molecular players. To date, any such mammary gland analyses have mostly focussed on later stages of development (pregnancy, lactation, involution) (D'Cruz *et al*., 2002; Master *et al*., 2002; Gass *et al*., 2003; Rudolph *et al*., 2003; Clarkson *et al*., 2004; Stein *et al*., 2004). Here we present an expression microarray time course analysis covering five stages of pubertal development, from the

Correspondence: Professor F Martin, UCD School of Biomolecular and Biomedical Science, Conway Institute, University College Dublin, Belfield, Dublin 4, Ireland.
E-mail: finian.martin@ucd.ie
[4]Current address: Department of Laboratory Medicine, Cell and Experimental Pathology, Lund University, Clinical Research Centre, Entrance 72, House 91, Floor 11, Malmö University Hospital, S-205 02 Malmö, Sweden.
Received 21 December 2006; revised 28 February 2007; accepted 9 March 2007; published online 7 May 2007

appearance to the regression of TEBs. We highlight members of the Wnt, transforming growth factor-β (TGFβ) and oestrogen signalling pathways, which potentially contribute to mammary gland development at this time. We compare our findings from normal development with those of altered pubertal development in the CITED1 knockout (KO) mouse. Our results implicate CITED1 as a co-regulator of oestrogen signalling during puberty and suggest that such signalling pathways are maintained in a subgroup of breast tumours in women exhibiting good prognosis.

Results

Expression microarray analysis of pubertal mammary gland development

To assess the timing of pubertal mammary gland development, we prepared wholemounts from 3- to 7-week-old mice. We consistently found ($n = 36$ mice examined) that TEBs were absent at 3 weeks, present at 4, 5 and 6 weeks and had regressed by 7 weeks. Representative wholemounts are shown in Figure 1a. Based on the wholemount analysis, these five time points (3, 4, 5, 6 and 7 weeks) were chosen for subsequent microarray analysis. The aim of the study was to assess gene expression changes associated with mammary gland development that accompanies the onset of puberty, that is that which reflects: (1) the advancement of the mammary tree through the fat pad and (2) the appearance to the disappearance of TEBs. Our wholemount analysis showed that using mammary glands from age-matched mice of 3–7 weeks would cover this activity. The disadvantage of our design is that mice in our later time points might be at different stages of the oestrus cycle and so exhibit heterogeneous gene expression. However, by sample pooling and integration of independent replicate pools, we derived 'representative' gene expression profiles that were unique to each time point and significantly different from all others (see Figure 1b, hierarchical clustering condition tree).

A total of 14 samples were hybridized to Affymetrix MOE430A arrays (each time point in triplicate except for 5 weeks which was in duplicate). Quality control hierarchical clustering of the 14 arrays, based on the expression of all 22 000 transcripts, clustered samples from the same time point together with the exception of one of the 4 week samples, which was only slightly misplaced (Figure 1b, condition tree). This confirmed that age was a prominent driver of gene expression. We have already seen that age reflects pubertal mammary gland development and ductal morphogenesis (Figure 1a). The cluster analysis also indicated that the expression profiles of 3 and 4 week samples were quite similar and distinct from those of 5, 6 and 7 week samples (Figure 1b, condition tree).

A master list ('pubertal genes') of 1126 probe sets representing 930 unique genes was identified, from which subsequent analysis was performed (Supplementary Data 1). Each of the pubertal genes was either upregulated or downregulated by at least twofold during pubertal mammary gland development (Figure 1b, gene tree). A trend was evident for genes to increase in expression from 3 and 4 weeks to 5, 6 and 7 weeks (Figure 1b, transition from blue to red). OntoExpress (Draghici *et al*., 2003) highlighted the following biological functions as being more prevalent than expected among the pubertal genes: growth factor activity, cell growth (cell proliferation and cell cycle genes), Wnt receptor signalling, metabolism (in particular fatty acid metabolism, proteolysis and peptidolysis) and catalysis (acyltransferase and oxidoreductase activity).

As an indication of data quality, the expression profiles of known mediators of pubertal mammary gland development were examined. Pubertal ductal morphogenetic dysfunction has been observed in mouse models with inhibition of amphiregulin (Areg), inhibin-βb (Inhbb), matrix metalloproteinases (Mmp2, Mmp3), E-cadherin (Cdh1), the transporter, Slc12a2 and prolactin receptor (Prlr) expression (Howlin *et al*., 2006a). Expression of all of these genes was found to increase in our data set (Figure 1c). Similarly, KO mice have shown that CITED1, possibly through regulation of oestrogen signalling, is a mediator of pubertal ductal outgrowth and our data confirmed the increase in expression of CITED1 during normal pubertal mammary gland development (Figure 1c; and Howlin *et al*., 2006b).

Comparison to parity-related gene expression changes

After puberty, in the absence of a subsequent pregnancy, the adult nulliparous gland retains a higher susceptibility to cancer than an age-matched parous gland (D'Cruz *et al*., 2002). A parity-associated signature of genes, that are either upregulated or downregulated in the age-matched parous versus nulliparous gland, has been identified and may be responsible for the differences in cancer susceptibility (D'Cruz *et al*., 2002). We used a method of unsupervised hierarchical clustering to group the 14 pubertal arrays based only on the expression of the 36 genes in the parity-associated gene signature. Significant differences in expression were seen, and these 36 genes alone were sufficient to cluster the arrays accurately by time point (Figure 1d). Such a clustering pattern was not seen using a group of 36 random genes (data not shown). The majority of genes that change with parity are initially upregulated during puberty between 4 and 5 weeks of age (Figure 1d).

'TEB profile' genes

Genes that were expressed or repressed specifically when TEBs were present were termed 'TEB profile' genes. That is, genes that were upregulated between 3 and 4 weeks and downregulated between 6 and 7 weeks (expressed when TEBs are present) and genes that were downregulated between 3 and 4 weeks and upregulated between 6 and 7 weeks (repressed when TEBs are present). We identified 15 expressed and 9 repressed 'TEB profile' genes (Figure 2). Functional analysis of the 'TEB profile' genes identified apoptosis and cell cycle

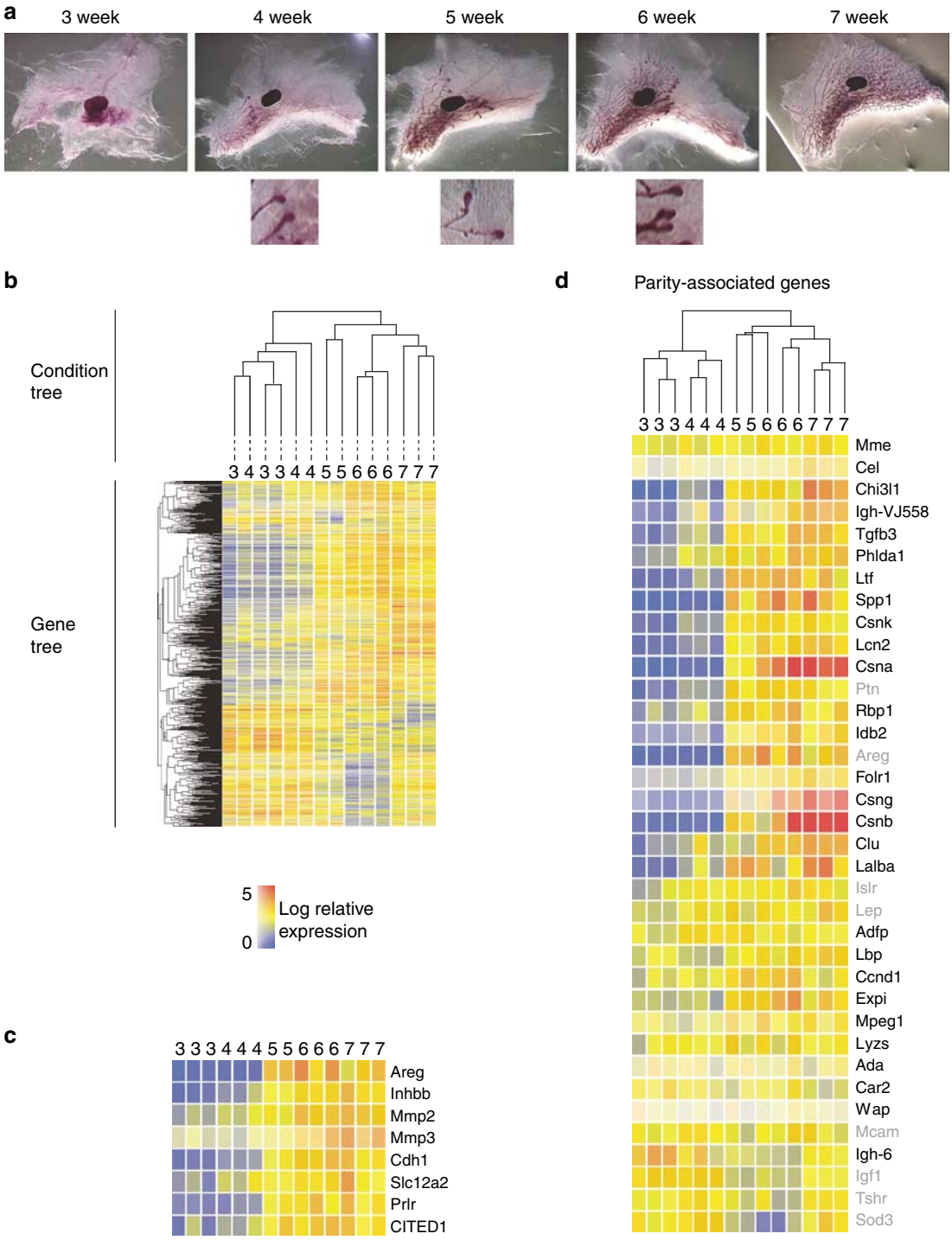

Figure 1 Microarray analysis of pubertal mammary gland development. (**a**) Pubertal mammary gland wholemounts at 3, 4, 5, 6 and 7 weeks. Close-up images are shown below the wholemounts where TEBs are present. ×8 Magnification. (**b**) Hierarchical clustering of arrays into a condition tree based on the expression of all genes (>22 000). Heat map showing expression of 930 pubertal genes across 14 arrays. Rows represent probe sets; columns represent arrays with time points indicated above in weeks. Gene tree was generated by hierarchical clustering based on gene expression across all 14 arrays. Blue represents low expression, yellow intermediate and red high expression. (**c**) Expression profiles of eight known mediators of pubertal mammary gland development. Columns represent arrays with time points listed above in weeks. Rows represent genes with the same colour coding as b. (**d**) Heat map showing expression of 36 parity-associated genes. Hierarchical clustering grouped the arrays into a condition tree based only on the expression of these 36 genes. Gene names are listed on the right. Genes that are upregulated with parity are printed in black; genes downregulated with parity are printed in grey.

A

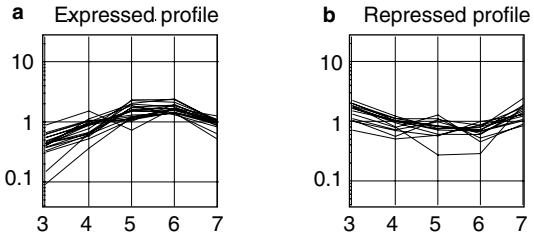

B

Symbol	Gene Name	Apoptosis /cell cycle regulation
Expressed genes		
Cdc2a	cell division cycle 2, homolog A	yes
Cnn1	calponin 1	
Egr2	early growth response 2	yes
Ehf	ets homologous factor	
Gsta3	glutathione S-transferase, alpha 3	
Igfbp2	insulin-like growth factor binding protein 2	yes
Ly6d	lymphocyte antigen 6 complex, locus D	
Mup1	major urinary protein 1	
Myh11	myosin heavy polypeptide 11, smooth muscle	yes
Rnf149	ring finger protein 149	
Sdc1	syndecan 1	yes
Sfrp1	secreted frizzled-related sequence protein 1	yes
Tgif	TG interacting factor	yes
Tns1	tensin 1	
Tnfrsf12a	tumour necrosis factor receptor superfamily, 12a	yes
Repressed genes		
Coro1a	coronin, actin binding protein 1a	
Ets1	E26 avian leukemia oncogene 1, 5' domain	yes
Gsn	gelsolin	yes
Igh-6	immunoglobulin heavy chain 6	
Lck	lymphocyte protein tyrosine kinase	yes
Nrip1	nuclear receptor interacting protein 1	
Phgdh	3-phosphoglycerate dehydrogenase	
Tcra	T-cell receptor alpha chain	yes
Tcrb-v13	T-cell receptor beta, variable 13	yes

Figure 2 TEB profile genes. (**A**) Graphs showing the expressed and repressed 'TEB profiles' of gene expression. (a) The normalized expression levels of 15 genes increased by $\geqslant$1.5-fold between 3 and 4 weeks and decreased by $\geqslant$1.5-fold between 6 and 7 weeks. (b) The normalized expression levels of nine genes decreased by $\geqslant$1.5-fold between 3 and 4 weeks and increased by $\geqslant$1.5-fold between 6 and 7 weeks. *X* axis: time points (weeks), *y* axis: log-relative expression. (**B**) Table listing the 15 expressed and 9 repressed 'TEB profile' genes. Genes with known roles in apoptosis or cell cycle regulation are noted.

regulation as overrepresented functions with more than half of the genes belonging to these categories (Figure 2). This is in strong agreement with findings of Morris *et al*. (2006) who studied genes specifically expressed in TEBs relative to ductal tissue and found that 57% of TEB-specific genes had roles in cell cycle regulation, DNA replication or cell division (Morris *et al*., 2006). TEBs are also known to possess the highest levels of programmed cell death relative to all other stages of mammary gland development (Humphreys *et al*., 1996). Individually, several of the 'TEB profile' genes have previously been associated with pubertal mammary gland development, including gelsolin, igfbp2 and members of the Ets family of transcription factors (Crowley *et al*., 2000; Allar and Wood, 2004; Galang *et al*., 2004).

*Wnt, TGF*β *and oestrogen associated gene expression*

Functional analysis of the pubertal genes, based on Gene Ontology terms, identified 13 genes involved in Wnt receptor signalling (Supplementary Data 2). This is more than would be expected by chance in a group of genes of this size ($P<0.001$, OntoExpress). An enrichment of Wnt gene expression in TEBs has previously been reported, indicating a potential role for Wnt signalling during pubertal mammary gland development (Kouros-Mehr and Werb, 2006).

Comparison of the pubertal genes to a database of TGFβ-responsive genes (http://actin.ucd.ie/tgfbeta) identified 286 TGFβ-responsive genes with changing expression profiles during pubertal mammary gland development (Supplementary Data 3). The frequency of TGFβ-responsive genes among the pubertal genes is significantly higher than would be expected in a random group of genes of this size ($P<0.0001$) and implies the potential importance of TGFβ signalling during pubertal mammary gland development.

Most prominently, comparison of the pubertal genes to a database of oestrogen-responsive genes (Tang *et al*., 2004) identified 122 oestrogen-responsive genes with changing expression profiles during pubertal mammary

Table 1 Oestrogen-responsive pubertal genes

Symbol	*Name*	*Trajectory*	*ERE?*	*CITED1 KO*
Functional category: growth factor/growth factor receptor				
Areg	**Amphiregulin**	**FIFD**	**Yes**	**Down**
Erbb3	v-erb-b2 erythroblastic leukemia viral oncogene homolog 3	FIIF	No	Up
Fgfr2	Fibroblast growth factor receptor 2	FIFF	N/A	
Inhbb	Inhibin beta-B	IIFF	Yes	
Kdr	Kinase insert domain Protein receptor	FFFF	No	
Kit	Kit oncogene	IFFF	Yes	Down
Tgfb3	Transforming growth factor, beta 3	IIFF	No	Down
Functional category: cell growth and maintenance				
Ccnb1	Cyclin B1	FFFD	Yes	Down
Fabp4	Fatty acid binding protein 4, adipocyte	FDFF	No	Up
Fhl1	Four and a half LIM domains 1	FDIF	N/A	
Gadd45a	Growth arrest and DNA-damage-inducible 45 alpha	IFFF	No	
Gas1	Growth arrest specific 1	IIFF	Yes	
Igfbp2	Insulin-like growth factor binding protein 2	IIFD	Yes	Down
Igfbp4	Insulin-like growth factor binding protein 4	FDFF	Yes	
Igfbp5	Insulin-like growth factor binding protein 5	FFFF	Yes	
Il1r2	**Interleukin 1 receptor, type II**	**FFFF**	**No**	**Up**
Kcnk2	Potassium channel, subfamily K, member 2	FDFF	No	
Lcn2	Lipocalin 2	IIFF	Yes	
Pttg1	Pituitary tumor-transforming 1	FFFD	No	
Slc12a2	Solute carrier family 12, member 2	IFFI	No	
Slc2a1	Solute carrier family 2 (facilitated glucose transporter), member 1	FIFF	No	
Socs2	Suppressor of cytokine signaling 2	FFIF	No	
Ube2c	Ubiquitin-conjugating enzyme E2C	FFFD	Yes	
Functional category: development				
Actg2	Actin, gamma 2, smooth muscle, enteric	FIFD	Yes	
Cd8a	CD8 antigen, alpha chain	FDIF	No	Up
Cyr61	Cysteine rich protein 61	IDFF	Yes	
Itgav	Integrin alpha V	FFFF	No	Down
Ndn	Necdin	FDFF	No	
Sfrp1	Secreted frizzled-related sequence protein 1	IIFD	Yes	Up
Sfrp2	Secreted frizzled-related sequence protein 2	FFFF	No	
Thbs1	**Thrombospondin 1**	**FIIF**	**No**	**Down**
Thbs2	Thrombospondin 2	FIFD	No	Down
Timp1	Tissue inhibitor of metalloproteinase 1	FIFD	No	
Tnfrsf12a	Tumor necrosis factor receptor superfamily, member 12a	IIFD	No	
Wnt5a	Wingless-related MMTV integration site 5A	FFFF	No	Up
Functional category: signal transduction				
Adm	Adrenomedullin	IFFF	No	
Anxa3	Annexin A3	FFFF	No	
Ceacam1	CEA-related cell adhesion molecule 1	IIFF	Yes	
Cxcl14	Chemokine (C-X-C motif) ligand 14	IIFF	Yes	Down
F3	Coagulation factor III	FIFD	No	
Gabrp	Gamma-aminobutyric acid (GABA-A) receptor, pi	IFFF	No	
Gfra1	Glial cell line derived neurotrophic factor family receptor alpha 1	IIFD	Yes	
Grb10	Growth factor receptor bound protein 10	FDFI	Yes	
Pik3r1	Phosphatidylinositol 3-kinase regulatory subunit polypeptide 1	FFFI	No	Down
Prlr	Prolactin receptor	FIFF	No	
Stc2	**Stanniocalcin 2**	**IIFF**	**Yes**	**Down**
Tacstd2	Tumor-associated calcium signal transducer 2	IIFF	Yes	
Functional category: transcription factor/nucleic acid binding				
Bcl6	B-cell leukemia/lymphoma 6	FFFF	Yes	
Bhlhb2	Basic helix–loop–helix domain containing, class B2	FFFF	No	
Egr2	**Early growth response 2**	**IIFD**	**No**	

Table 1 (*continued*)

Symbol	*Name*	*Trajectory*	*ERE?*	*CITED1 KO*
Ehf	Ets homologous factor	IIID	No	
Elf1	E74-like factor 1	FFIF	No	
Fos	**FBJ osteosarcoma oncogene**	**FIFF**	**Yes**	**Up**
Foxp1	Forkhead box P1	FFFF	Yes	
Hes1	Hairy and enhancer of split 1 (*Drosophila*)	FFFF	No	
Hmgb2	High mobility group box 2	FFFD	No	
Irf6	Interferon regulatory factor 6	IIFF	Yes	
Irx5	Iroquois related homeobox 5 (*Drosophila*)	FIFF	No	
Jun	Jun oncogene	FIFF	No	
Myb	Myeloblastosis oncogene	IIIF	Yes	Up
Nfatc3	Nuclear factor of activated T-cells, cytoplasmic 3	FFDI	Yes	
Nfia	Nuclear factor I/A	DFFF	Yes	Up
Nfil3	Nuclear factor, interleukin 3, regulated	FIFI	Yes	
Nrip1	Nuclear receptor interacting protein 1	DFDI	Yes	
Runx1	Runt related transcription factor 1	FIFF	No	
Sfpq	Splicing factor proline/glutamine rich	FFDI	Yes	
Sfrs10	Splicing factor, arginine/serine-rich 10	FFDI	No	
Sox9	SRY-box containing gene 9	IIDI	No	
Tcf7	Transcription factor 7, T-cell specific	DFII	Yes	
Tgfb1i4	Transforming growth factor beta 1 induced transcript 4	FFFF	Yes	
Trps1	Trichorhinophalangeal syndrome I (human)	IIFF	No	Up
Ubtf	Upstream binding transcription factor, RNA polymerase I	FFFI	Yes	
Functional category: catalytic activity				
Ccnd2	Cyclin D2	FFDI	No	
Cdkn1a	Cyclin-dependent kinase inhibitor 1A (P21)	DFFF	Yes	
Cp	Ceruloplasmin	FDFI	Yes	
Dpysl3	Dihydropyrimidinase-like 3	FIDI	Yes	
Impdh2	Inosine 5′-phosphate dehydrogenase 2	FIFF	No	
Ptprk	Protein tyrosine phosphatase, receptor type, K	FIFF	No	
Rab5c	RAB5C, member RAS oncogene family	FFDI	Yes	
Rgs2	Regulator of G-protein signaling 2	DFFF	No	
Functional category: metabolism				
Acly	ATP citrate lyase	IDDI	Yes	Up
Apod	Apolipoprotein D	FIFD	No	
Cdc2a	Cell division cycle 2 homolog A	IFFD	No	Down
Clu	Clusterin	FFFF	Yes	
Comt	Catechol-*O*-methyltransferase	IFFF	Yes	
Csnk2a1	Casein kinase II, alpha 1 polypeptide	FFDI	Yes	
Dusp6	Dual specificity phosphatase 6	FIFD	Yes	
Fen1	Flap structure specific endonuclease 1	FIFF	Yes	Down
Gzma	Granzyme A	FIFF	Yes	Up
Idh2	isocitrate dehydrogenase 2	FFFF	Yes	
Lpl	Lipoprotein lipase	FDFF	Yes	
Pam	Peptidylglycine alpha-amidating monooxygenase	DFID	No	Up
Phgdh	**3-phosphoglycerate dehydrogenase**	**DFFF**	**No**	**Down**
Phlda1	Pleckstrin homology-like domain, family A, member 1	IFFF	No	
Plat	Plasminogen activator, tissue	FIFF	Yes	
Plod2	Procollagen lysine, 2-oxoglutarate 5-dioxygenase 2	FFFD	Yes	
Rpl27a	Ribosomal protein L27a	FFDI	No	Down
Rps6ka3	Ribosomal protein S6 kinase polypeptide 3	FDFF	No	
Scd1	Stearoyl-Coenzyme A desaturase 1	IFFI	Yes	
Functional category: other				
Cd24a	CD24a antigen	FIFF	Yes	Up
Cdh11	Cadherin 11	FIFF	No	Up
Cldn4	Claudin 4	FIFF	Yes	
Csng	Casein gamma	FIII	No	Down
Cspg2	Chondroitin sulfate Proteoglycan 2	FIFD	No	
Efemp1	EGF-containing fibulin-like ECM protein 1	IFFF	No	Up
Fxyd2	FXYD domain-containing ion transport regulator 2	FIFF	Yes	
H2-Aa	Histocompatibility 2, class II antigen A, alpha	FFFF	Yes	
H2-Eb1	Histocompatibility 2, class II antigen E, beta	IIFF	No	
Hccs	Holocytochrome c synthetase	FDFF	Yes	
Ier3	Immediate early response 3	FFFF	No	
Ifit3	Interferon-induced protein with tetratricopeptide repeats 3	FFFD	No	
Ii	Ia-associated invariant chain	FFFF	Yes	
Kcnj8	Potassium inwardly rectifying channel, subfamily J member 8	FFFF	No	
Krt1-19	Keratin complex 1, acidic, gene 19	IIFF	No	

Table 1 (*continued*)

Symbol	*Name*	*Trajectory*	*ERE?*	*CITED1 KO*
Ltf	Lactotransferrin	IIFF	Yes	Down
Myh11	Myosin heavy chain 11, smooth muscle	IFFD	Yes	
Pawr	PRKC, apoptosis, WT1, regulator	FIIF	No	
Ptx3	**Pentraxin related gene**	**FIFF**	**No**	**Up**
Slc9a3r1	Solute carrier family 9 isoform 3 regulator 1	FFFF	Yes	
Tnc	Tenascin C	IIFD	No	
Tpbg	Trophoblast glycoprotein	FIFF	No	
Wbp5	WW domain binding protein 5	FFFF	Yes	

Abbreviations: ERE, oestrogen-response element; KO, knockout; RT–PCR, reverse transcription–polymerase chain reaction. Gene symbol and name are provided for 122 oestrogen-responsive pubertal genes listed by functional category. Trajectory describes the expression profile from 3 to 7 weeks where expression changes from week to week are indicated as increasing (I), decreasing (D) or remaining flat (F). The presence (yes) or absence (no) of an ERE within 5000 bp upstream of the transcription start site is noted. N/A indicates that sequence was not available. Regulation of gene expression in CITED1 KO mice relative to controls is described as upregulated (up), downregulated (down) or blank if no regulation was seen. The pubertal expression profiles of genes listed in bold were verified by real-time RT–PCR analysis.

gland development (Table 1). The apparent change in the expression level of this number of oestrogen-responsive genes in the total cohort of genes that changed is significantly greater than that expected by chance ($P = 0.0035$) (Figure 3a). As the post-pubertal time point samples were pools and not selected for stage of the oestrus cycle, this may not accurately represent, but only estimate, the actual number of oestrogen-responsive genes that are upregulated in the mammary gland over this period. The expression profiles of eight of these oestrogen-responsive pubertal genes were confirmed by real-time reverse transcription–polymerase chain reaction (RT–PCR) analysis (Figure 3b). Sequence analysis of two of the gene sequences, stanniocalcin2 (Stc2) and Areg, identified one putative oestrogen-response element (ERE) downstream of the transcription start site in both of these genes (Figure 3c). Chromatin immunoprecipitation (ChIP) analysis demonstrated that an anti-ERα antibody successfully precipitated the regions of DNA containing these EREs in 6-week mammary glands (Figure 3c). The specificity of the antibody binding to this region was confirmed by amplification of an independent region of the Stc2 promoter that does not contain an ERE (Figure 3c, control). Thus, the oestrogen responsiveness of Stc2 and Areg during puberty is most likely regulated by direct ERα binding to specific EREs in these genes.

The Wnt, TGFβ and oestrogen-signalling pathways are all known targets for transcriptional co-regulation by CITED1 (Yahata *et al*., 2001; Plisov *et al*., 2005). We have previously identified gene expression changes associated with the loss of CITED1 by comparing expression levels between 6-week CITED1 KO and control mammary glands (Howlin *et al*., 2006b). Cross comparison of the data sets identified several members of the Wnt, TGFβ and oestrogen-signalling pathways, which have altered expression levels in CITED1 KO mice relative to controls (Supplementary Data 2, 3 and Table 1). CITED1 KO mice display reduced ductal outgrowth, altered branch patterning and a reduced number of TEBs during puberty (Figure 4A; Howlin *et al*., 2006b). The comparative gene expression data therefore support the building evidence for an important role for Wnt, TGFβ and oestrogen signalling in normal pubertal mammary gland development as well as a potential role for CITED1 in regulating these pathways.

Co-regulation of pubertal gene expression by ERα and CITED1

To consider the potential involvement of CITED1 solely in modulating oestrogen signalling in the pubertal mammary gland, we compared the cellular localization of CITED1 and ERα. Both proteins, in agreement with previous reports, were expressed in some but not all epithelial cells of the ducts in an on/off pattern (Zeps *et al*., 1998; Howlin *et al*., 2006b). ERα appeared nuclear, while CITED1 was predominantly cytoplasmic and weakly nuclear. Interestingly, both proteins were expressed in exactly the same ductal cells and absent from the same cells (Figure 4Ba). Supplementary Data 4 show immunofluorescence images in xy and yz planes to support the 2D confocal images shown in Figure 4Ba. Nuclear colocalization of ERα and CITED1 is apparent from these images. This staining pattern provides additional suggestive evidence of an interaction between ERα and CITED1. ERα staining in the CITED1 KO mammary gland appeared comparable with that in the wild-type (wt) gland (Figure 4Bb).

In wt TEBs, cap cells expressed neither ERα nor CITED1 (Figure 4Bd). In the body cells, however, both proteins were expressed in an on/off pattern similar to that seen in the ducts. ERα expression appeared to be dispersed throughout the body cells of the TEB. CITED1, however, displayed a gradient of expression with strong expression in the outermost body cells (closest to the cap cell layer) and little or no expression in the inner body cells (closest to the lumen). Thus, ERα and CITED1 localized to the same outermost body cells, but those body cells closest to the lumen expressed ERα with little or no CITED1 (Figure 4Bd).

The body cells closest to the lumen have been reported to undergo extensive apoptosis (Humphreys *et al*., 1996). As these cells express little or no CITED1, we questioned whether the location of apoptotic cells would be altered in CITED1 KO mice, where CITED1

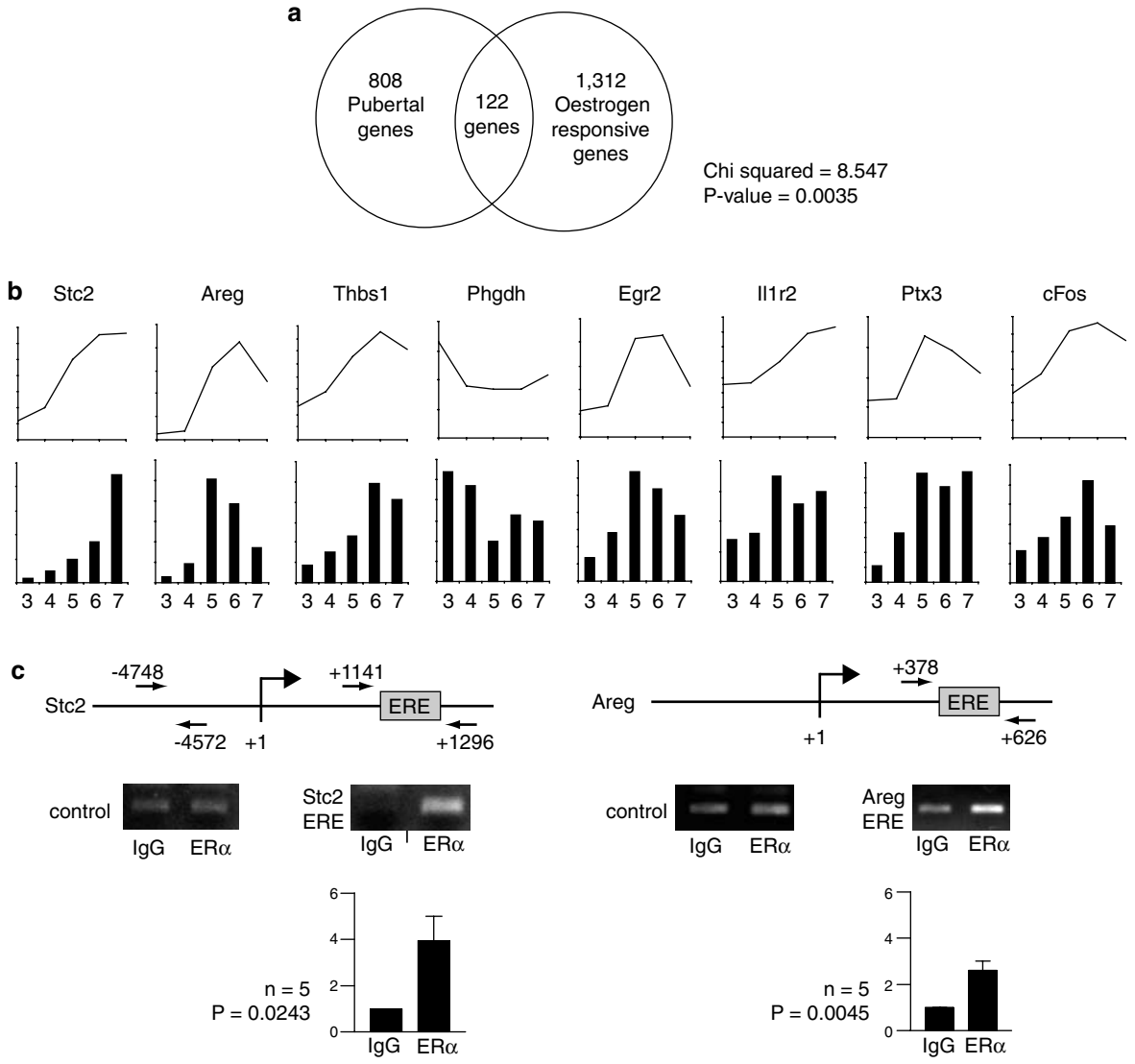

Figure 3 Expression of oestrogen-responsive genes. (**a**) Venn diagram: comparison of the 930 pubertal genes with 1434 oestrogen-responsive genes from ERGDB. One hundred and twenty-two genes belong to both groups. This is significantly more than would be expected by chance ($P=0.0035$). (**b**) Relative expression profiles for eight oestrogen-responsive genes: stc2, areg, thbs1, phgdh, egr2, il1r2, ptx3 and cfos. Line graphs (top) show the expression profiles determined by microarray analysis. Bar graphs (bottom) show confirmation of these expression profiles as determined by real-time RT–PCR. *X* axis: time points (weeks); *y* axis: mean relative expression ($n=2$). (**c**) ChIP analysis of 6-week mammary glands. Diagrams represent Stc2 and Areg genes with location of EREs. Arrows indicate position of primers. Transcription start sites are marked as +1. Representative images of PCR results show, for both genes, specific immunoprecipitation of an ERE-containing region of DNA with anti-ERα antibody. Quantitative PCR results show significant differences when compared with immunoprecipitation with normal IgG. Samples were equally loaded and results normalized to inputs. Comparison is also made to amplification of a non-ERE-containing region of DNA (control).

was absent from all body cells. Immunofluorescence determined that the apoptotic marker, cleaved caspase 3, was located predominantly in the inner body cells of TEBs of the CITED1 KO mice (Figure 4Ca). The localization and extent of this staining is consistent with previous observations of both cleaved caspase 3 and terminal deoxy transferase uridine triphosphate nick end-labeling staining in TEBs of wt mice (Humphreys *et al*., 1996; Mailleux *et al*., 2007). This would suggest that CITED1 knockout is not associated with gross changes in apoptosis. We observed similar expression patterns of cleaved caspase 3 in the ducts of wt and CITED1 KO mice, where occasional ductal cells displayed nuclear cleaved caspase 3 expression (Figure 4Cb–c). Ductal cells undergoing apoptosis tended to be those adjacent to ERα-positive cells and did not express ERα themselves (Figure 4C). Thus, the reduced ductal outgrowth and reduced number of TEBs observed in the 6-week-old CITED1 KO mice do not appear to be due to differences in apoptosis between wt and CITED1 KO mice.

To further examine the effect of loss of CITED1 on oestrogen-signalling pathways, the expression of the oestrogen-responsive pubertal genes Stc2 and Areg was

confirmed in wt and CITED1 KO mice by real-time RT–PCR analysis (Figure 4D). Expression was compared between 3- and 6-week glands using typical underdeveloped CITED1 KO glands and also particularly well developed CITED1 KO glands (6d), which exhibited a similar extent of ductal outgrowth to the wt.

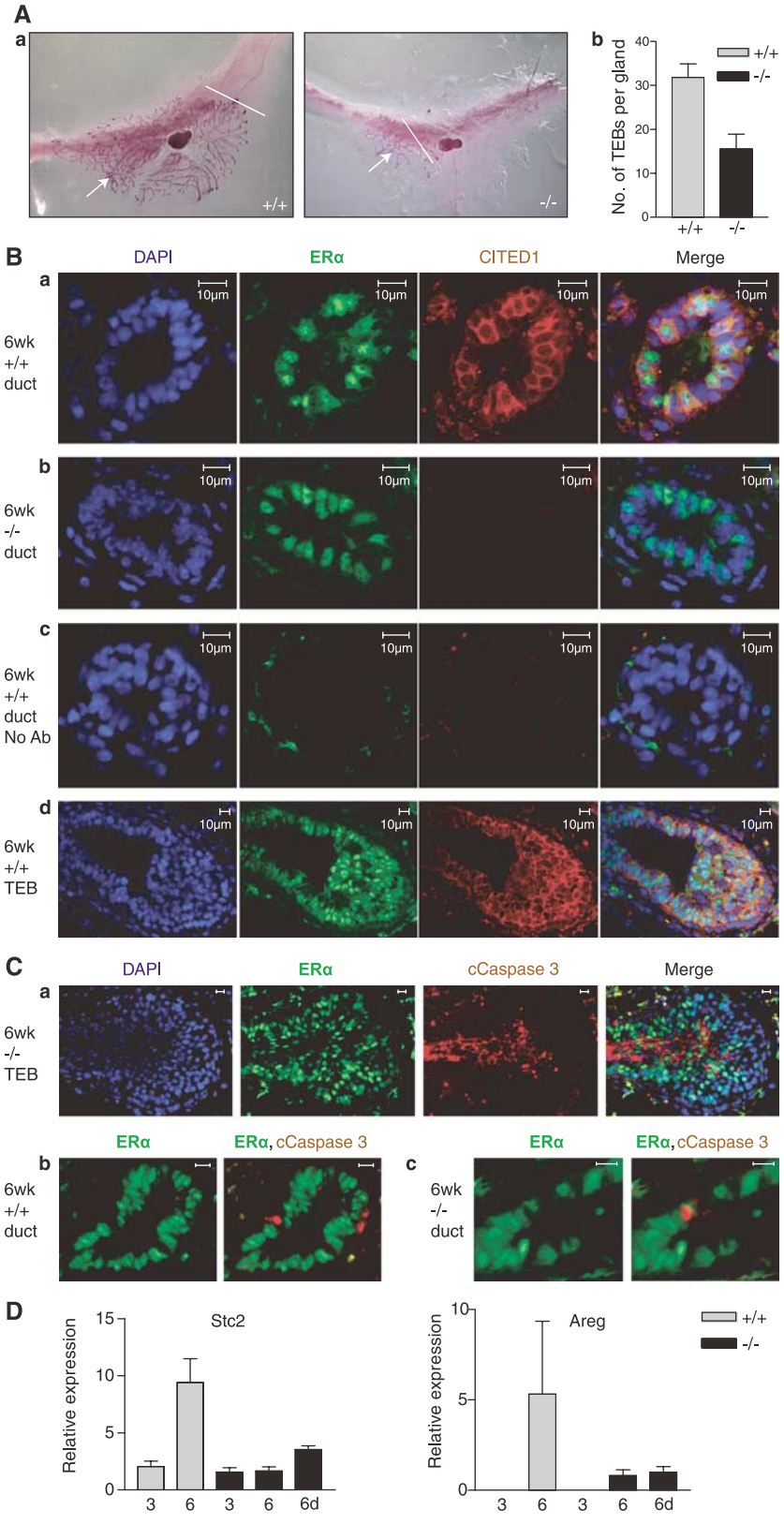

For both genes, the increase in expression between 3 and 6 weeks, clearly seen in the wt glands, was either absent or considerably reduced in the CITED1 KO glands. This trend was present despite the stage of development of the KO gland, although it was more pronounced in the less well-developed gland. This observation of disrupted oestrogen signalling in CITED1 KO mice further supports the theory of a co-regulatory interaction between ERα and CITED1.

Relating mouse pubertal development to human cancer progression

As ERα expression is associated with outcome of human breast cancer, it became a matter of interest to see if the co-regulatory events observed in pubertal mouse mammary gland development were also observed in human breast tumours. We considered the expression microarray study carried out by van de Vijver *et al*. (2002). Expression profiles were derived from the primary tumours of 295 patients, and follow-up information is available for 18.2 years (median: 6.7 years) (van de Vijver *et al*., 2002). Dividing the patients into groups based on the expression of CITED1 in these tumours, we found a significant correlation between high CITED1 expression levels and both event-free survival and overall survival ($P<0.05$ and <0.01, respectively) (Figure 5a). The expression of CITED1 correlated positively with the expression of ERα in these tumours ($P<0.0001$). Additionally, the expression of CITED1 positively correlated with expression of Areg ($P=0.0002$), Stc2 ($P<0.0001$) and Stc1 ($P<0.0001$) (Figure 5b). These data suggest that an ERα–CITED1 co-regulated signalling pathway may be maintained in some breast tumours and may be an indicator of good prognosis.

Discussion

We have provided a comprehensive gene expression data set for the period of pubertal mammary gland development from the appearance to the regression of TEBs. Our global time course analysis of the entire gland differs from the approach of other research groups who have looked at a single pubertal time point and compared isolated segments of the gland (Kouros-Mehr and Werb, 2006; Morris *et al*., 2006). While the different approaches complement each other and a degree of overlap was apparent between findings, we identify both key global trends of pubertal development as well as dynamic expression changes for novel genes, not previously associated with pubertal mammary gland development.

The 'TEB profile' genes provide a novel list of pubertal genes that also play possible roles in breast cancer progression. Reports have shown high levels of ehf and tnfrsf12a in breast tumours (Galang *et al*., 2004; Michaelson *et al*., 2005). Cdc2a levels are known to increase in response to carcinogen treatment in the virgin mammary gland (Uehara *et al*., 2006). Expression of syndecan1 can promote breast carcinoma growth (Maeda *et al*., 2006). Igfbp2 can be used as a marker for anti-oestrogen-resistant breast cancer cell lines (Juncker-Jensen *et al*., 2006). Calponin1 can be used to distinguish invasive from non-invasive breast lesions (Werling *et al*., 2003). A loss of sfrp1, a Wnt inhibitor, is associated with breast cancer progression and poor prognosis, as is the presence of Ets1 (Klopocki *et al*., 2004; Lincoln and Bove, 2005). These findings indicate the potential relationship between understanding the mechanisms of normal developmental programmes and gaining understanding of oncogenic growth.

Accumulating evidence indicates that hyperactive Wnt signalling occurs in association with the development and progression of human breast cancer (Yook *et al*., 2006). Wnt signalling pathway members identified here, such as Wnt2, Wnt5a and Fzd1, have previously been observed in the pubertal mammary gland (Weber-Hall *et al*., 1994; Kouros-Mehr and Werb, 2006). Members of the Wnt family are thought to act as paracrine mediators of progesterone signalling during pregnancy but, to date, a clear role has not been established for Wnts during puberty (Brisken *et al*., 2000). A number of TGFβ-signalling pathway members have also been implicated in the progression of breast cancer. For example, pleiotrophin, a proto-oncogene identified in our study, is expressed at high levels in breast cancer (Zhang *et al*., 1997). TGFβ is known to be a potent inhibitor of mammary epithelial proliferation and is believed to play an important role in branch patterning during normal pubertal development,

Figure 4 CITED1 and oestrogen receptor signalling. (**A**) (a) Representative wholemounts of 6 week wt (left) and CITED1 KO (right) glands ($n=126$). Ductal outgrowth is significantly reduced in CITED1 KO glands, $P<0.0005$. (b) Bar graph showing the significantly lower mean number of TEBs in 6-week CITED1 KO (black) glands relative to wt (grey) ($n=20$, $P=0.0022$). (**B**) Confocal fluorescent microscopy of sections through 6-week glands. (a) Wt duct (b) CITED1 KO duct (c) wt duct negative control with no primary antibodies (d) wt TEB. ERα (green) displays nuclear staining in some but not all of the ductal epithelial cells in an on/off pattern. CITED1 (red) is predominantly cytoplasmic and weakly nuclear, and is located in some but not all of the ductal epithelial cells in an on/off pattern. Merged image shows that ERα and CITED1 localized to the same ductal cells. In TEBs, ERα is located in body cells but absent from cap cells. CITED1 is located in body cells, particularly the outermost body cells and absent from cap cells. Merged image shows CITED1 and ERα localize to the same outermost body cells. Body cells closest to the lumen express ERα but only weakly express CITED1. (**C**) Fluorescent microscopy of sections through 6-week glands. (a) CITED1 KO TEB stained for nuclear DAPI (blue), ERα (green) and cleaved caspase 3 (red). Cleaved caspase 3 staining is both nuclear and cytoplasmic and is confined to the inner body cells of the TEB and the presumptive luminal space. (b) Wt duct and (c) CITED1 KO duct, both stained for ERα (green) and cleaved caspase 3 (red). Cleaved caspase 3 was found only in occasional ductal cells. Ductal cells that stained positively for cleaved caspase 3 did not express ERα. Scale bars 10 μm. (**D**) Expression of oestrogen-responsive pubertal genes, Stc2 and Areg, measured by real-time RT–PCR in 3- and 6-week wt and CITED1 KO glands ($n=3$). Exceptionally, well-developed 6-week CITED1 KO glands showing a similar extent of ductal outgrowth as the wt glands were also analysed (6d).

although details of its signalling mechanism have yet to be clearly defined.

Many of the genes whose expression levels increase during puberty retain elevated expression levels at the end of puberty. Several of these genes have known roles in pregnancy and/or lactation (e.g. Prlr, casein family members). Thus, this expression trend reflects the role of puberty as a preparatory step for later mammary development and not as an isolated process in itself. This can also be seen by the comparison with parity-induced changes, where many of the genes that are upregulated at puberty are further upregulated with parity (Figure 1d; D'Cruz *et al*., 2002). However, there are also a number of genes whose expression levels remain high at the end of puberty, which are preserved in the mature virgin gland, but which decrease with parity (e.g. Areg, CITED1). It has previously been reported that Areg expression may contribute to abnormal development in the older, mature mammary gland (Herrington *et al*., 1997). Owing to the growth promoting effects exhibited by both Areg and CITED1 (Howlin *et al*., 2006b), it is conceivable that the high level of expression of these genes may contribute to the increased susceptibility of the nulliparous gland to cancer (Kenney *et al*., 1996; D'Cruz *et al*., 2002; Howlin *et al*., 2006b).

The growth promoting effects of CITED1 may be mediated through modulation of oestrogen signalling as oestrogen is known to promote proliferation in the pubertal mouse mammary gland (Zeps *et al*., 1998). The localization of CITED1 and ERα to exactly the same epithelial cells of the pubertal mammary gland lends credence to the possibility of an interaction between these two proteins. Similarly, the downregulation of oestrogen-responsive genes in CITED1 KO mice implies that CITED1 does modulate oestrogen-signalling pathways. The mechanism by which CITED1 and ERα may interact in the pubertal mammary gland remains unclear. The predominantly cytoplasmic location of CITED1 may be a result of exportin 1 (CRM-1)-dependent nuclear export, but does not exclude the possibility of an interaction between CITED1 and ERα in the nucleus (Shi *et al*., 2006). Indeed, CITED1 has previously been shown to act as a co-activator of oestrogen-dependent transcription by binding directly to ERα, in an oestrogen-dependent manner (Yahata *et al*., 2001). The transcriptional activity of CITED1 has also been shown to be regulated by alterations in the phosphorylation status of CITED1 (Shi *et al*., 2006). Phosphorylation of CITED1 interferes with p300 binding (Shi *et al*., 2006). However, as p300 and ERα appear to interact with different regions of CITED1, it is not yet clear whether phosphorylation of CITED1 affects CITED1–ERα-binding ability (Yahata *et al*., 2001).

The potential interaction between CITED1 and ERα is limited to some of the body cells of the TEB. CITED1 expression appears to be lost from the inner body cells, closest to the lumen. We have not examined the mechanisms of CITED1 loss but have only considered the potential consequences of this expression pattern. Inner and outer body cells undergo varying levels of proliferation and apoptosis with proliferation tending to localize to the outer body cells (Humphreys *et al*., 1996). It has been shown, in both mouse and human tissue, that proliferating cells tend to be those adjacent

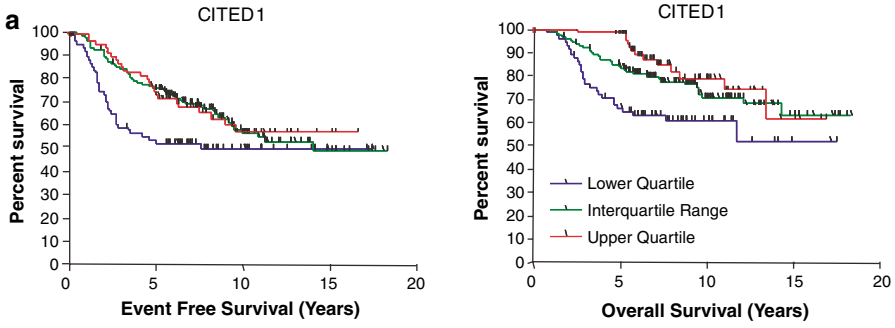

b Correlation with CITED1 gene expression:

	Pearson r	p-value	Significant?
ERα	0.441	<0.0001	Yes
Areg	0.2119	0.0002	Yes
Stc2	0.3195	<0.0001	Yes
Stc1	0.246	<0.0001	Yes

Figure 5 Pubertal genes in breast cancer. (**a**) Kaplan–Meier curves for event-free survival (left) and overall survival (right). A total of 295 patients were divided into three groups based on CITED1 expression levels: red, upper quartile; green, interquartile range; blue, lower quartile. The lower quartile had significantly poorer outcomes for both event-free survival ($P<0.05$) and for overall survival ($P<0.01$). (**b**) Pearson correlations between CITED1 expression and expression of other pubertal genes in the same cohort of 295 breast tumours. Significant positive correlations were found with ERα, Areg, Stc2 and Stc1.

to ERα-positive cells (Clarke *et al*., 1997; Zeps *et al*., 1998). As ERα-positive cells are distributed throughout the body cells of the TEB, we speculate that CITED1 may be involved in co-regulating the oestrogen-induced proliferation of the outer body cells and may contribute to the differences in proliferation rate seen between this latter cell type and inner body cells.

The role of CITED1 as an indicator of good prognosis in breast cancer may appear to contradict the role of CITED1 as a promoter of pubertal growth. However, this observation is mirrored in the case of ERα, which also promotes pubertal growth and acts as an indicator of good prognosis in breast tumours. CITED1 expression in breast tumours correlated with expression of ERα and also those of Areg and Stc2. This suggests that tumours, in which pathways relevant to normal mammary physiology and development are maintained, may have a significantly better patient outcome than those tumours in which these pathways have been lost. This observation is consistent with the well-established correlation between low tumour grade (histological similarity to normal breast) and good outcome, and with a recent study showing that breast tumours with gene expression profiles most similar to differentiated mammary acini in culture, have a favourable prognosis (Fournier *et al*., 2006). While we have demonstrated a relationship between pathways in development and cancer, it is clear that it is not as straightforward as might be expected. Growth factors promoting developmental invasive behaviour may not be assumed to promote cancerous invasion and may, paradoxically, by their expression in a tumour, indicate maintenance of a more regulated and controlled growth.

In conclusion, expression microarray analysis has highlighted novel genes involved in pubertal mammary gland development with potential relevance to breast cancer susceptibility and progression. Our analysis emphasizes the importance of an ERα–CITED1 co-regulated signalling mechanism in puberty and, interestingly, retention of this pathway may be indicative of good prognosis in human breast cancer.

Materials and methods

Animals and tissue isolation
CD1 mice were euthanized at various stages of development (3, 4, 5, 6 and 7 weeks of age). CITED1 KO mice were bred and genotyped as described previously (Howlin *et al*., 2006b). Fourth inguinal mammary glands were isolated and either snap frozen in liquid nitrogen, fixed in appropriate fixative or used immediately for ChIP analysis. Lymph nodes were removed from glands used for microarray and ChIP analysis. CITED1 KO glands harvested for RNA had contralateral glands fixed as wholemounts to give an indication of the extent of ductal outgrowth.

Wholemount analysis
Glands were fixed and stained in carmine alum as described previously (Howlin *et al*., 2006b). TEBs were counted in 10 representative wholemounts from each genotype. Unpaired *t*-test was used for statistical comparison of the means.

Immunofluorescence
Immunofluorescence was performed essentially as described previously (Howlin *et al*., 2006b) Primary antibodies used were: rabbit polyclonal anti-CITED1 1:500 (Li *et al*., 1998), mouse monoclonal anti-ERα 1:50 (Novocastra Laboratories, Newcastle upon Tyne, UK) and rabbit monoclonal anti-cleaved caspase 3 (Cell Signaling Technology, Danvers, MA, USA). DAPI (4,6-diamidino-2-phenylindole dihydrochloride, Sigma, St Louis, MO, USA, 0.0001%) was used as a nuclear counterstain. Images were captured using a fluorescent microscope with Axiovision LE software or a Zeiss LSM 510 UVMETA confocal microscope and Zeiss LSM software.

Microarray hybridization and data analysis
Total RNA (6 μg) was used to produce biotinylated cRNA according to the manufacturer's instructions (Affymetrix, High Wycombe, UK). Each sample was prepared from a pool of at least three mice, and a total of 15 samples were prepared (three replicates for each of five time points: 3, 4, 5, 6 and 7 weeks of age). Insufficient cRNA was obtained for one of the 5-week replicates, so this time point was analysed in duplicate. Affymetrix test3 arrays were used to confirm the quality of the labelled cRNA before hybridization to the Affymetrix MOE430A arrays. Raw data were imported into Genespring (version 5.0, Agilent Technologies, Santa Clara, CA, USA) and normalization was performed by per chip normalized to the 50th percentile and per gene normalized to the median. A filtering step was applied to select reliable data (probe sets that were flagged as present in seven of 14 time points), and also changing data (determined by twofold changes in normalized expression intensities between any two time points). Trajectory clustering (Phang *et al*., 2003) was performed based on 1.5-fold expression changes between consecutive time points where I is $\geqslant$1.5-fold increase in expression, D is $\geqslant$1.5-fold decrease in expression and F is anything in between. Hierarchical clustering was performed using a Pearson correlation with selected gene groups. The parity-associated gene group was extracted from the published gene signature based on gene symbols (D'Cruz *et al*., 2002). Functional categories were determined based on Gene Ontology categories. *P*-values were calculated using OntoExpress default settings (hypergeomatric distribution, fdr correction), with P-value <0.05 considered to be significant. TGFβ and oestrogen-responsive gene comparisons were made based on gene symbols using the T-REGs database of TGFβ-responsive genes (http://actin.ucd.ie/tgfbeta/) and the ERGDB (Estrogen Responsive Genes Database: http://defiant.i2r.a-star.edu.sg/projects/Ergdb-v2/index.htm) (Tang *et al*., 2004). Statistical significance was calculated by χ^2 tests based on the assumption that the Affymetrix chips represented 14 000 mouse genes including all genes in the ERGDB and T-REGs databases. Statistical significance for Kaplan–Meier curves was calculated using the log-rank test. Expression microarray analysis of the CITED1 KO mice has been described previously (Howlin *et al*., 2006b). Gene lists were generated based on 1.5-fold expression changes between homozygous null (−/−) and control mice (either wt or heterozygous). The entire puberty data set, which is compliant to the MIAME criteria, is deposited at Gene Expression Omnibus (GEO, http://www.ncbi.nlm.nih.gov/geo/) under the series accession number GSE6453.

ChIP analysis
Dragon ERE finder was used to identify putative EREs (Bajic *et al*., 2003). A ChIP assay kit (Upstate Biotechnology, Billerica, MA, USA) was used according to the manufacturer's instructions and essentially as we have described previously

(Murtagh *et al*., 2004). A detailed protocol is provided as Supplementary Data 5. The primary antibody used was: rabbit polyclonal anti-ERα (SantaCruz TransReagent, 5 μl). Normal rabbit serum (5 μl) was used as a control.

Real-time PCR

SYBR Green PCR was performed essentially as described previously (Howlin *et al*., 2006b) with the following primers: Areg forward 5′-GACTCACAGCGAGGATGACA-3′ and reverse 5′-CTGTGATAACGATGCCGATG-3′; Stc2 forward 5′-GACCCTCTGGAAGCAGTGAG-3′ and reverse 5′-ACA CATCCAGCGTGTGACAT-3′; Thbs1 forward 5′-GTCTCC ATGGTCGTCCTGTT-3′ and reverse 5′-TTTCTTGCAGGC TTTGGTCT-3′; Phgdh forward 5′-GACCCCATCATCTCT CCTGA-3′ and reverse 5′-GCACACCTTTCTTGCACTGA-3′; Egr2 forward 5′-AGTTGGGTCTCCAGGTTGTG-3′ and reverse 5′-GGAGATCCAGGGGTCTCTTC-3′; Il1r2 forward 5′-GCATCATTGGGGTCAAGACT-3′ and reverse 5′-TGAG TACTGGGGGTGTAGCC-3′; Ptx3 forward 5′-GTGGGTG GAAAGGAGAACAA-3′ and reverse 5′-GGCCAATCTG TAGGAGTCCA-3′; cFos forward 5′-CCAGTCAAGAGCA TCAGCAA-3′ and reverse 5′-AGTACAGGTGACCACGG GAG-3′ and β-actin forward 5′-GCTACAGCTTCACCAC CACA-3′ and reverse 5′-AAGGAAGGCTGGAAAAGAGC-3′. Relative expression values were normalized to β-actin expression levels. Real-time PCR Taqman assay was used for analysis of immunoprecipitated DNA from ChIP analysis as detailed in Supplementary Data 5.

Acknowledgements

We thank Joseph Mooney of the Biomedical Facility, Alison Murphy and Catherine Moss of the Conway Institute Core Facility, UCD, for their technical assistance. This work was supported by grants from Science Foundation Ireland, IRCSET, Ireland, and the Health Research Board, Ireland.

References

Allar MA, Wood TL. (2004). Expression of the insulin-like growth factor binding proteins during postnatal development of the murine mammary gland. *Endocrinology* **145**: 2467–2477.

Bajic VB, Tan SL, Chong A, Tang S, Strom A, Gustafsson JA *et al*. (2003). Dragon ERE Finder version 2: a tool for accurate detection and analysis of estrogen response elements in vertebrate genomes. *Nucleic Acids Res* **31**: 3605–3607.

Ball SM. (1998). The development of the terminal end bud in the prepubertal-pubertal mouse mammary gland. *Anat Rec* **250**: 459–464.

Brisken C, Heineman A, Chavarria T, Elenbaas B, Tan J, Dey SK *et al*. (2000). Essential function of Wnt-4 in mammary gland development downstream of progesterone signaling. *Genes Dev* **14**: 650–654.

Clarke RB, Howell A, Potten CS, Anderson E. (1997). Dissociation between steroid receptor expression and cell proliferation in the human breast. *Cancer Res* **57**: 4987–4991.

Clarkson RW, Wayland MT, Lee J, Freeman T, Watson CJ. (2004). Gene expression profiling of mammary gland development reveals putative roles for death receptors and immune mediators in post-lactational regression. *Breast Cancer Res* **6**: R92–R109.

Crowley MR, Head KL, Kwiatkowski DJ, Asch HL, Asch BB. (2000). The mouse mammary gland requires the actin-binding protein gelsolin for proper ductal morphogenesis. *Dev Biol* **225**: 407–423.

D'Cruz CM, Moody SE, Master SR, Hartman JL, Keiper EA, Imielinski MB *et al*. (2002). Persistent parity-induced changes in growth factors, TGF-beta3, and differentiation in the rodent mammary gland. *Mol Endocrinol* **16**: 2034–2051.

Daniel C, Silberstein G. (2000). *Methods in Mammary Gland Biology and Breast Cancer Research*. Kluwer Academic/Plenum Publishers: New York.

Draghici S, Khatri P, Bhavsar P, Shah A, Krawetz SA, Tainsky MA. (2003). Onto-Tools, the toolkit of the modern biologist: Onto-Express, Onto-Compare, Onto-Design and Onto-Translate. *Nucleic Acids Res* **31**: 3775–3781.

Fournier MV, Martin KJ, Kenny PA, Xhaja K, Bosch I, Yaswen P *et al*. (2006). Gene expression signature in organized and growth-arrested mammary acini predicts good outcome in breast cancer. *Cancer Res* **66**: 7095–7102.

Galang CK, Muller WJ, Foos G, Oshima RG, Hauser CA. (2004). Changes in the expression of many Ets family transcription factors and of potential target genes in normal mammary tissue and tumors. *J Biol Chem* **279**: 11281–11292.

Gass S, Harris J, Ormandy C, Brisken C. (2003). Using gene expression arrays to elucidate transcriptional profiles underlying prolactin function. *J Mammary Gland Biol Neoplasia* **8**: 269–285.

Herrington EE, Ram TG, Salomon DS, Johnson GR, Gullick WJ, Kenney N *et al*. (1997). Expression of epidermal growth factor-related proteins in the aged adult mouse mammary gland and their relationship to tumorigenesis. *J Cell Physiol* **170**: 47–56.

Howlin J, McBryan J, Martin F. (2006a). Pubertal mammary gland development: insights from mouse models. *J Mammary Gland Biol Neoplasia* **11**: 283–297.

Howlin J, McBryan J, Napoletano S, Lambe T, McArdle E, Shioda T *et al*. (2006b). CITED1 homozygous null mice display aberrant pubertal mammary ductal morphogenesis. *Oncogene* **25**: 1532–1542.

Humphreys RC, Krajewska M, Krnacik S, Jaeger R, Weiher H, Krajewski S *et al*. (1996). Apoptosis in the terminal endbud of the murine mammary gland: a mechanism of ductal morphogenesis. *Development* **122**: 4013–4022.

Juncker-Jensen A, Lykkesfeldt AE, Worm J, Ralfkiaer U, Espelund U, Jepsen JS. (2006). Insulin-like growth factor binding protein 2 is a marker for antiestrogen resistant human breast cancer cell lines but is not a major growth regulator. *Growth Horm IGF Res* **16**: 224–239.

Kenney NJ, Smith GH, Rosenberg K, Cutler ML, Dickson RB. (1996). Induction of ductal morphogenesis and lobular hyperplasia by amphiregulin in the mouse mammary gland. *Cell Growth Differ* **7**: 1769–1781.

Klopocki E, Kristiansen G, Wild PJ, Klaman I, Castanos-Velez E, Singer G *et al*. (2004). Loss of SFRP1 is associated with breast cancer progression and poor prognosis in early stage tumors. *Int J Oncol* **25**: 641–649.

Kouros-Mehr H, Werb Z. (2006). Candidate regulators of mammary branching morphogenesis identified by genome-wide transcript analysis. *Dev Dyn* **235**: 3404–3412.

Li H, Ahmed NU, Fenner MH, Ueda M, Isselbacher KJ, Shioda T. (1998). Regulation of expression of MSG1 melanocyte-specific nuclear protein in human melanocytes and melanoma cells. *Exp Cell Res* **242**: 478–486.

Lincoln II DW, Bove K. (2005). The transcription factor Ets-1 in breast cancer. *Front Biosci* **10**: 506–511.

Maeda T, Desouky J, Friedl A. (2006). Syndecan-1 expression by stromal fibroblasts promotes breast carcinoma growth *in vivo* and stimulates tumor angiogenesis. *Oncogene* **25**: 1408–1412.

Mailleux AA, Overholtzer M, Schmelzle T, Bouillet P, Strasser A, Brugge JS. (2007). BIM regulates apoptosis during mammary ductal morphogenesis, and its absence reveals alternative cell death mechanisms. *Dev Cell* **12**: 221–234.

Master SR, Hartman JL, D'Cruz CM, Moody SE, Keiper EA, Ha SI *et al*. (2002). Functional microarray analysis of mammary organogenesis reveals a developmental role in adaptive thermogenesis. *Mol Endocrinol* **16**: 1185–1203.

Michaelson JS, Cho S, Browning B, Zheng TS, Lincecum JM, Wang MZ *et al*. (2005). Tweak induces mammary epithelial branching morphogenesis. *Oncogene* **24**: 2613–2624.

Morris JS, Stein T, Pringle MA, Davies CR, Weber-Hall S, Ferrier RK *et al*. (2006). Involvement of axonal guidance proteins and their signaling partners in the developing mouse mammary gland. *J Cell Physiol* **206**: 16–24.

Murtagh J, McArdle E, Gilligan E, Thornton L, Furlong F, Martin F. (2004). Organization of mammary epithelial cells into 3D acinar structures requires glucocorticoid and JNK signaling. *J Cell Biol* **166**: 133–143.

Phang TL, Neville MC, Rudolph M, Hunter L. (2003). Trajectory clustering: a non-parametric method for grouping gene expression time courses, with applications to mammary development. *Pac Symp Biocomput* **8**: 351–362.

Plisov S, Tsang M, Shi G, Boyle S, Yoshino K, Dunwoodie SL *et al*. (2005). Cited1 is a bifunctional transcriptional cofactor that regulates early nephronic patterning. *J Am Soc Nephrol* **16**: 1632–1644.

Rudolph MC, McManaman JL, Hunter L, Phang T, Neville MC. (2003). Functional development of the mammary gland: use of expression profiling and trajectory clustering to reveal changes in gene expression during pregnancy, lactation, and involution. *J Mammary Gland Biol Neoplasia* **8**: 287–307.

Russo J, Moral R, Balogh GA, Mailo D, Russo IH. (2005). The protective role of pregnancy in breast cancer. *Breast Cancer Res* **7**: 131–142.

Shi G, Boyle SC, Sparrow DB, Dunwoodie SL, Shioda T, de Caestecker MP. (2006). The transcriptional activity of CITED1 is regulated by phosphorylation in a cell cycle-dependent manner. *J Biol Chem* **281**: 27426–27435.

Stein T, Morris JS, Davies CR, Weber-Hall SJ, Duffy MA, Heath VJ *et al*. (2004). Involution of the mouse mammary gland is associated with an immune cascade and an acute-phase response, involving LBP, CD14 and STAT3. *Breast Cancer Res* **6**: R75–R91.

Tang S, Han H, Bajic VB. (2004). ERGDB: Estrogen Responsive Genes Database. *Nucleic Acids Res* **32**: D533–D536.

Uehara N, Unami A, Kiyozuka Y, Shikata N, Oishi Y, Tsubura A. (2006). Parous mammary glands exhibit distinct alterations in gene expression and proliferation responsiveness to carcinogenic stimuli in Lewis rats. *Oncol Rep* **15**: 903–911.

van de Vijver MJ, He YD, van't Veer LJ, Dai H, Hart AA, Voskuil DW *et al*. (2002). A gene-expression signature as a predictor of survival in breast cancer. *N Engl J Med* **347**: 1999–2009.

Weber-Hall SJ, Phippard DJ, Niemeyer CC, Dale TC. (1994). Developmental and hormonal regulation of Wnt gene expression in the mouse mammary gland. *Differentiation* **57**: 205–214.

Werling RW, Hwang H, Yaziji H, Gown AM. (2003). Immunohistochemical distinction of invasive from noninvasive breast lesions: a comparative study of p63 versus calponin and smooth muscle myosin heavy chain. *Am J Surg Pathol* **27**: 82–90.

Williams JM, Daniel CW. (1983). Mammary ductal elongation: differentiation of myoepithelium and basal lamina during branching morphogenesis. *Dev Biol* **97**: 274–290.

Yahata T, Shao W, Endoh H, Hur J, Coser KR, Sun H *et al*. (2001). Selective coactivation of estrogen-dependent transcription by CITED1 CBP/p300-binding protein. *Genes Dev* **15**: 2598–2612.

Yook JI, Li XY, Ota I, Hu C, Kim HS, Kim NH *et al*. (2006). A Wnt-Axin2-GSK3beta cascade regulates Snail1 activity in breast cancer cells. *Nat Cell Biol* **8**: 1398–1406.

Zeps N, Bentel JM, Papadimitriou JM, D'Antuono MF, Dawkins HJ. (1998). Estrogen receptor-negative epithelial cells in mouse mammary gland development and growth. *Differentiation* **62**: 221–226.

Zhang N, Zhong R, Wang ZY, Deuel TF. (1997). Human breast cancer growth inhibited *in vivo* by a dominant negative pleiotrophin mutant. *J Biol Chem* **272**: 16733–16736.

Supplementary Information accompanies the paper on the Oncogene website (http://www.nature.com/onc).